Vol 18 No 11, November 2009
1674-1056/2009/18(11)/4882–06

Chinese Physics B

Investigation of the limit of lateral beam shifts on symmetrical metal-cladding waveguide*

Chen Lin(陈 麟)[a)†], Zhu Yi-Ming(朱亦鸣)[a)‡], Zhang Da-Wei(张大伟)[a)], Cao Zhuang-Qi(曹庄琪)[b)], and Zhuang Song-Lin(庄松林)[a)]

[a)] *Shanghai Key Lab of Modern Optical System, University of Shanghai for Science and Technology, Shanghai* 200093, *China*
[b)] *Guided Wave Photonics Group, Shanghai Jiao Tong University, Shanghai* 200240, *China*

(Received 28 February 2009; revised manuscript received 25 March 2009)

This paper reports that Goos–Hänchen (GH) shifts occurring on a symmetrical metal-cladding waveguide are experimentally identified. It was found that there exists a critical thickness of the upper metal layer, h_{cr}, above which negative shift is observed and reversely, positive shift occurs. Both positive and negative GH shifts near critical thickness do not vary dramatically and can achieve maximum with submillimeter scale, which is different from simulated results by using stationary-phase method. It also shows that this critical thickness, h_{cr}, can be obtained at the position for zero reflectivity by setting the intrinsic damping to be the same as the radiative damping. The GH effects observed near critical thickness are produced by extremely distortion of the reflected beam profiles, which limits the amplitude of GH shift and further the sensitivity of GH optical sensor based on the symmetrical metal-cladding waveguide.

Keywords: Goos–Hänchen shift, symmetrical metal-cladding waveguide, optical sensing
PACC: 4225G, 4282

1. Introduction

The Goos–Hänchen (GH) shift, which refers to the lateral shifts of beam position when light beam totally reflects from a boundary between two semi-infinite dielectric media, was first experimentally demonstrated by Goos and Hänchen.[1,2] In the case of two layers structure (one interface), the magnitude of GH shift is of the order of incident wavelength. To enlarge the magnitude, various structures and materials have been proposed theoretically[3–8] and experimentally.[9,10] Recently, it was recognised that the beam shifts reflected from a symmetrical metal-cladding waveguide (SMCW) structures can be extremely enhanced. This large shift is due to coupling of the incident energy to a guided wave.[8] Such interesting effects have shown wide applications in optical communication[11,12] and optical sensing.[13,14]

Large GH shifts can achieve optical sensors with high resolution.[14] Theoretical analysis shows that there exists a critical thickness of upper metal layer, $h_{\rm cr}$, above which negative shift is observed and reversely, positive shift occurs. Up to now, experimentally measuring GH shifts near $h_{\rm cr}$ has been largely ignored, which is very important for GH optical sensor based on SMCW.

In this paper, the critical thickness of upper metal layer, $h_{\rm cr}$, is examined experimentally. Furthermore, we also deduce the analytical expression of $h_{\rm cr}$ by setting the intrinsic damping to be the same as the radiative damping. The value of $h_{\rm cr}$ obtained from theoretical calculation fits on the experimental result very well. Then beam shifts from SMCW (GH shifts) near $h_{\rm cr}$ were observed. The extreme GH shift for SMCW can achieve around 1 mm. We also find that the absolute GH shifts change slightly when h is close to critical value. The trend of experimental results is similar to the simulated results by using Gaussian-beam model and different with results from stationary-phase method. This is because reflected beam is strongly distorted and suppressed when the thickness of upper metal layer is close to $h_{\rm cr}$, which limits the amplitude

*Project supported by the Research Fund for Selecting and Training Excellent Young Teachers in Universities of Shanghai, Shanghai Municipal Education Commission (Grant No slg08006), "Chen Guang" project of Shanghai Municipal Education Commission and Shanghai Education Development Foundation (Grant No 09CG49), Dawn Project of Education Committee of Shanghai and Shanghai Education Development Foundation (Grant No 08SG48), Innovation Program of Shanghai Municipal Education Commission (Grant No 09YZ221), the Program from Shanghai Committee of Science and Technology (Grant No 09YZ221) and the Program from Shanghai Committee of Science and Technology, China (Grant Nos 07DZ22026 and 08ZR1415400).
†E-mail: linchen@usst.edu.cn
‡Corresponding author. E-mail: ymzhu@usst.edu.cn

of GH shift and further the sensitivity of GH optical sensor based on SMCW. The present insights on the maximum GH shift contribute to enhance the resolution of displacement sensor and solution sensor with SMCW.

2. Experiment

The structure of SMCW is illustrated in Fig.1. A dielectric slab with submillimeter scale (thickness d, dielectric constant ε_1) is sandwiched between two gold films. The upper metal layer (thickness h, dielectric constant ε_2) is coupling layer and the bottom metal layer (dielectric constant ε_2) serves as both substrate and reflecting panel. When a laser beam casts on the upper layer by free space coupling, a large part of energy couples into the guiding layer, which results in the attenuated total reflection (ATR) dips.

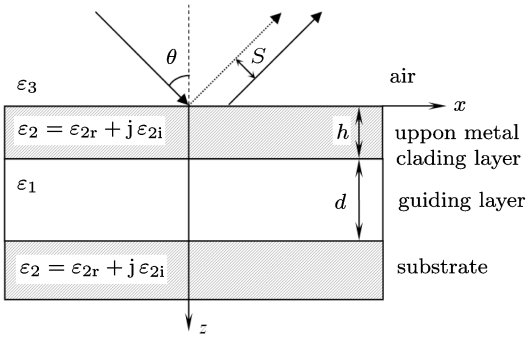

Fig.1. Schematic diagram of the SMCW.

By adjusting incident wavelength to let the component of wave-vector along the propagation direction coincide with the propagation constant of guided wave, the GH shift can be largely enhanced. This phenomenon can be explained by the reason that SMCW can strongly confine energy of guided wave in the guided layer.[15,16]

The experimental setup for measuring GH shifts near $h_{\rm cr}$ is shown in Fig.2. For fabricating an SMCW, an upper gold film (ε_2=–28+j1.8 at wavelength 860 nm) was sputtered onto the surface of a glass slab (d = 0.38 μm, ε_1 = 2.278). A 3000 nm-thick gold film was sputtered at the back side. A collimated light beam, after passing through TE-passed-polarizer, irradiates the upper metal layer of the SMCW. At first we use a photodiode to detect the reflected beam. Then, operating angle (θ=7.93°) for maximum GH shift can be selected when the reflectivity of the light near the certain dip of the spectrum reaches the maximum. After the angle is fixed, photodiode is moved out of the light path and the reflected beam directly incidents on the position sensitive detector (PSD). Precise wavelength is controlled by a temperature cell.

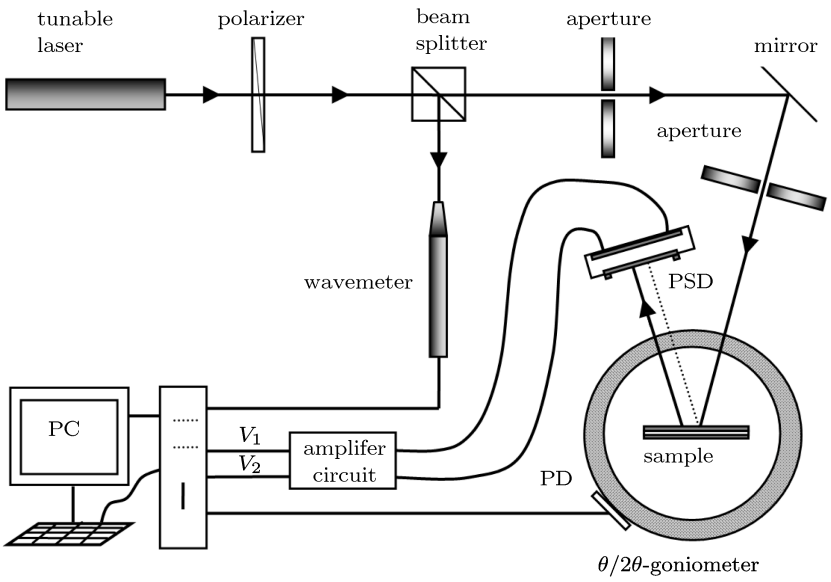

Fig.2. Experimental setup for measuring GH shifts.

Figure 3 represents the measured beam shifts S as a function of wavelength for various thicknesses of upper gold films h from 27 nm to 34 nm. Positive shifts are obtained when h=27.8, 29.1 and 29.9 nm, and negative shifts occur when h = 33.5, 31.7 and 31.2 nm. Then the critical thickness, $h_{\rm cr}$, can be obtained from 29.9 nm to 31.2 nm from the experiment. In Subsection 3.1, we will deduce the analytical formula of the critical thickness, $h_{\rm cr}$, which will be compared with experimental results. In addition, when the thickness h is a little bit less than $h_{\rm cr}$, positive displacements can reach more than 800 μm, i.e., maximum positive shifts for h = 27.8, 29.1 and 29.9 nm are 724, 847 and 563 μm, respectively. When the thickness h exceeds the critical value, negative shifts, which can reach above 100 μm, do not change dramatically. The maximum negative shifts for h = 33.5, 31.7 and 31.2 nm are –176, –181 and –153 μm, respectively. In Subsection 3.2, we will use the stationary-phase method and Gaussian-beam model to simulate GH shifts for comparison and discuss the difference between theoretical and experimental results in detail.

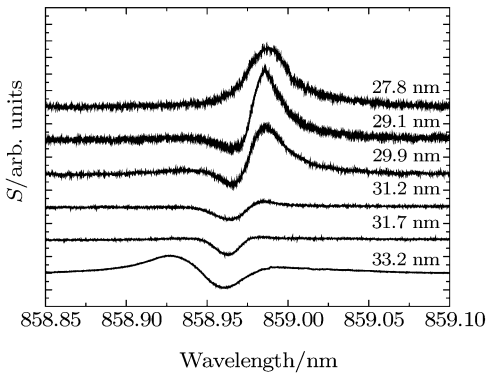

Fig.3. Contrastive graph of experimental results of GH shifts S versus incident wavelength with various h.

3. Discussion

3.1. The determination of critical thickness

In this subsection we will derive the critical thickness, $h_{\rm cr}$, for zero reflectivity. Firstly, we use the weak coupling condition to deduce the analytical expressions of intrinsic damping and radiative damping. Then by setting the intrinsic damping to be the same as the radiative damping, the expression of critical thickness, $h_{\rm cr}$, for zero reflectivity is obtained.

Figure 4 shows four types of metal cladding waveguides. Figure 4(a) is a structure of three-layer metal cladding waveguide without considering intrinsic damping, which comes from metal loss, and radiative damping. Figure 4(b) is a structure of three-layer metal cladding waveguide only with considering intrinsic damping. By using three-layer waveguide theory, for TE mode, we can express the propagation constant, $\beta^{4\rm a}$, of guided modes for three-layer metal cladding waveguide without considering the metal absorption as

$$\beta^{4a} = \frac{\pi}{\lambda d}\sqrt{4\varepsilon_1 d^2 - (m_0\lambda)^2}, \tag{1}$$

where λ is incident wavelength and m_0 is mode order. Comparing Fig.4(a) with Fig.4(b) under the condition of $|\varepsilon_{2\rm r}| \gg \varepsilon_{2\rm i}$ at visible and near infrared wavelength ($\varepsilon_{2\rm r}$ and $\varepsilon_{2\rm i}$ are real and imaginary parts of dielectric constant ($\varepsilon_2 = \varepsilon_{2\rm r} + {\rm j}\varepsilon_{2\rm i}$)), we can obtain that metal loss only affects the imaginary part of propagation constant in three-layer metal cladding waveguide. Then the intrinsic damping, ${\rm Im}(\beta^0)$, can be written as

$${\rm Im}(\beta^0) = \frac{\varepsilon_{2\rm i}k_0^2(\kappa_1^{4\rm a})^2}{\alpha_2^{4\rm a}(\kappa_1^{4\rm a} + (\alpha_2^{4\rm a})^2)\beta^{4\rm a}d_{\rm eff}} \tag{2}$$

with

$$\kappa_1^{4\rm a} = \sqrt{k_0^2\varepsilon_1 - (\beta^{4\rm a})^2}, \tag{3}$$

$$\alpha_2^{4\rm a} = \sqrt{(\beta^{4\rm a})^2 - k_0^2\varepsilon_{2\rm r}}, \tag{4}$$

and

$$d_{\rm eff} = d + 2/\alpha_2^{4\rm a}, \tag{5}$$

where $\alpha_2^{4\rm a}$ is the absorption constant of the cladding layer, $\kappa_1^{4\rm a}$ is the vertical guiding wave vector of three-layer metal cladding waveguide without considering the metal absorption, and $d_{\rm eff}$ is the effective thickness, $k_0 = 2\pi/\lambda$ is the wave-number in vacuum, β_0 is the eigen-propagation constant of the guided mode for three-layer waveguide with semi-infinite-thick coupling layer (see Fig.4(b)).

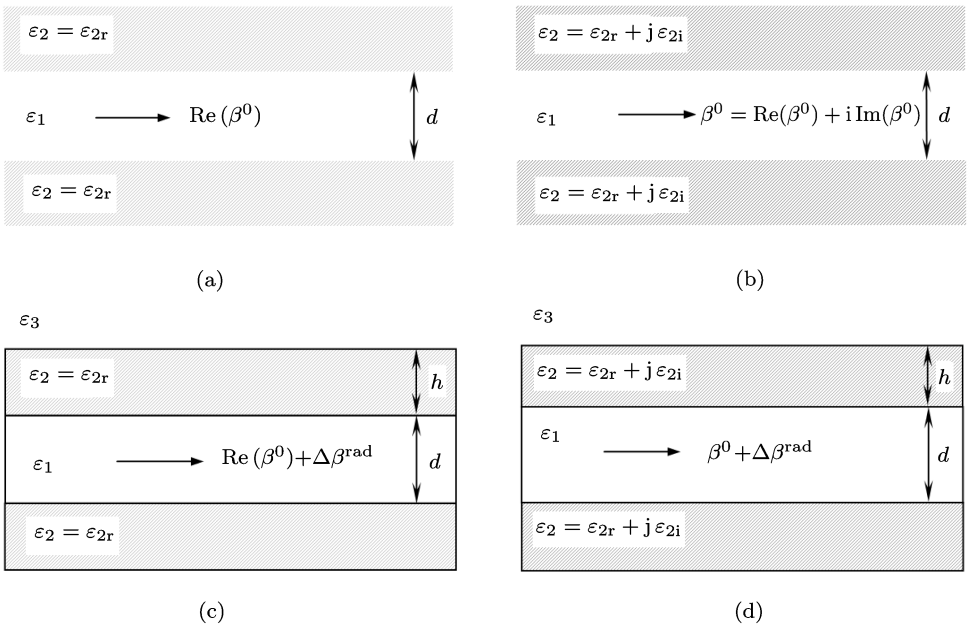

Fig.4. (a) Three-layer metal cladding waveguide with $\varepsilon_2 = \varepsilon_{2r}$ and $h \to \infty$; (b) three-layer metal cladding waveguide with $\varepsilon_2 = \varepsilon_{2r} + \mathrm{j}\varepsilon_{2i}$ and $h \to \infty$; (c) symmetrical metal cladding waveguide with $\varepsilon_2 = \varepsilon_{2r}$ and $h \neq \infty$; (d) symmetrical metal cladding waveguide with $\varepsilon_2 = \varepsilon_{2r} + \mathrm{j}\varepsilon_{2i}$ and $h \neq \infty$.

Figure 4(c) is a structure of SMCW only with considering radiative damping. Comparing Fig.4(c) with Fig.4(a) by using weak-coupling condition, which is satisfied with four-layer system,[17] we can express the radiative damping, $\mathrm{Im}(\Delta\beta^{\mathrm{rad}})$ as

$$\mathrm{Im}(\Delta\beta^{\mathrm{rad}}) = \frac{4\alpha_2^{4a}(\kappa_1^{4a})^2\kappa_3^{4a}\exp(-2\alpha_2^{4a}h)}{((\kappa_1^{4a})^2 + (\alpha_2^{4a})^2)((\kappa_3^{4a})^2 + (\alpha_2^{4a})^2)\beta^{4a}d_{\mathrm{eff}}} \tag{6}$$

with

$$\kappa_3^{4a} = \left(k_0^2\varepsilon_3 - \left(\beta^{4a}\right)^2\right)^{1/2}, \tag{7}$$

where $\Delta\beta^{\mathrm{rad}}$ represents the difference of the eigen-propagation constant between three-layer waveguide and free space coupling system (see Fig.4(d)). Because the radiative damping is inversely proportional to the exponential function of h as shown in Eq.(6), the radiative damping can be adjusted by changing the parameter h.

The critical thickness, h_{cr}, for zero reflectivity can be determined by setting Eq.(6) to be the same as Eq.(2), and simplified as

$$h_{\mathrm{cr}} = \frac{\lambda}{4\pi\kappa}\ln\frac{2}{n}, \tag{8}$$

where n and κ are the complex refractive indexes of metal ($n + \mathrm{j}\kappa = (\varepsilon_2)^{1/2}$). From Eq.(8) we can see that h_{cr} is determined by metal permittivity and incident wavelength. This property implies that h_{cr} only depends on the intrinsic damping. By using the parameters $\varepsilon_2 = -28 + \mathrm{j}1.8$ and $\lambda = 859$ nm, we can obtain $h_{\mathrm{cr}} = 31$ nm. The simulated result calculated by Eq.(8) fits on the experimental result very well.

3.2. Reflected field of a Gaussian beam from an SMCW structure

The experimental results shown in Fig.3 show that both positive and negative shifts do not change dramatically near critical thickness h_{cr}. For comparison, we also use the stationary phase method and Gaussian beam model to simulate GH shifts (with the same parameters for the experiment as shown in Fig.3), as shown in Figs.5(a) and 5(b), respectively. All the other parameters are the same as those in Fig.3. According to stationary phase method, when the thickness of the upper metal layer, h, approaches to h_{cr}, that is, the reflectivity becomes zero and the

radiative damping is the same as the intrinsic damping, the GH shift S should be infinity. However, in Gaussian-beam model, GH shifts remain finite and can achieve 1200 μm.

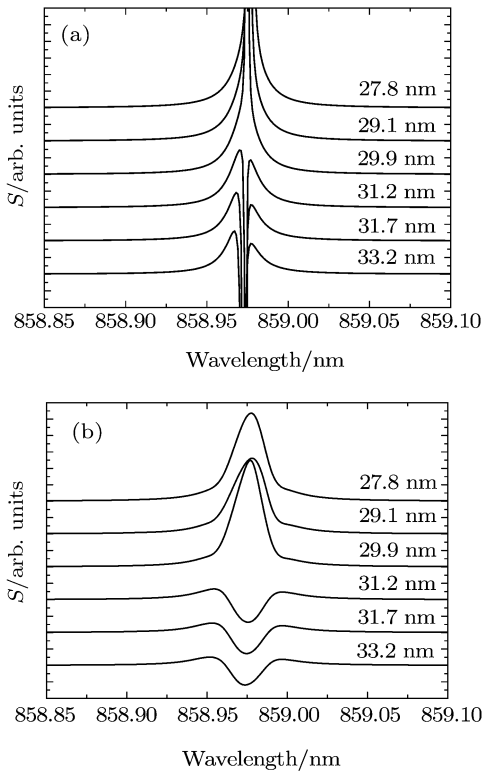

Fig.5. Theoretical calculation of GH shifts versus incident wavelength with various h by using (a) stationary phase method and (b) Gaussian-beam model (the waist radius for Gaussian simulation is assumed to be 800 μm).

From Fig.5(b), we can clearly see the difference of the GH shift between the stationary phase model and experimental results. Therefore, here, we calculate the field distribution of the reflected beam with different h by using the Gaussian beam model. Considering an incident beam of Gaussian shape

$$\psi_{\rm i}(x, z=0) = \frac{1}{\sqrt{2\pi}} \int A(\beta) \exp({\rm i}\,\beta x) {\rm d}\beta, \qquad (9)$$

we get the Fourier spectrum of the incident beam $A(\beta)$,

$$A(\beta) = w_x \exp\left[-(w_x^2/2)(\beta - \beta_{x0})^2\right], \qquad (10)$$

where $w_x = w_0 \sec\theta_0$, w_0 is the beam width at the waist. The field of the reflected beam is given by

$$\psi_{\rm r}(x, z=0) = \frac{1}{\sqrt{2\pi}} \int r(\beta) A(\beta) \exp({\rm i}\,\beta x) {\rm d}\beta. \qquad (11)$$

The integration above is extended over the interval $(-k_{\rm v}, k_{\rm v})$, where $k_{\rm v}$ is the wave vector in the vacuum. The calculated beam shift can be obtained by finding the location where $|\Psi_{\rm r}(x, z=0)|$ is maximum.[5]

Figure 6 shows the field distribution of the reflected beam with different h by using the Gaussian beam model. The lateral shift is determined by the location of the major peaks at the situations when almost all the field is focused on the peak and the reflected beam profile is close to Gaussian profile. When h is equal to the critical thickness, i.e., h=31 nm, a double peak occurs and the amplitude of left-hand peak is the same as that of right-hand peak. Furthermore, the peaks are smaller than that of the highest peaks for the other curves. When h gradually decreases, the radiative damping starts to enhance and exceeds the intrinsic damping. At this time, right-hand peak increases and left-hand peak decreases. The location of the right-hand major peaks are at the side of $x > 0$ and gradually move to the left side. The energy of beam starts to transfer from left-hand peak to right-hand peak. In this case, GH shift decreases and becomes positive. On the contrary, when h increases and exceeds the critical thickness, the radiative damping is smaller than the intrinsic damping. Under such condition, the left-hand peak starts to increase with the decrease of the right-hand peak. Meanwhile, the location of the left-hand major peaks is at the side of $x < 0$ and gradually shifts to the position of $x = 0$. In this case, GH shift is negative and the absolute value of GH shift decreases with increasing the thickness of the upper metal layer, h.

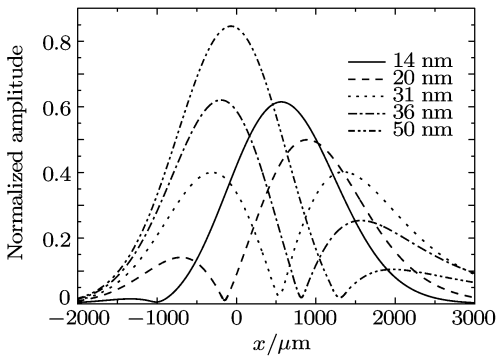

Fig.6. Field distribution of the reflected beam with various h (the waist radius for Gaussian simulation is assumed as 800 μm).

Therefore, when the GH shifts are located at the points with zero reflectivity, the reflected beam is effectively suppressed and distorted. The trend of the change of experimental results agrees with the numerical results very well. In addition, when the thickness

of the upper metal layer, h, is 29.1 nm and 29.9 nm, as seen in Fig.3, GH shifts, S, have a bipolar feature; i.e., an initial negative dip and a subsequent positive peak. This may be due to the multi-reflectivity effect. More detailed comparison between theory and experiment calls for further study.

4. Conclusion

The lateral beam shifts of the reflected beam from SMCW near the critical thickness of upper metal layer have been studied theoretically and experimentally. There exists the critical thickness of the upper metal layer on SMCW, above which negative shifts occur, and inversely positive shifts are observed. It is worth to be mentioned that the extreme GH shift from SMCW can achieve about 1 mm. We find that the GH shifts do not change dramatically at this critical condition. This is because reflected beam is strongly distorted and suppressed when the thickness of upper metal layer is close to $h_{\rm cr}$. Taking advantage of this experimental and theoretical study, invaluable information of GH shift from SMCW has been obtained. The present insights on the maximum GH shift contribute to enhance the resolution of displacement sensor and solution sensor with SMCW.

References

[1] Goos F and Hänchen H 1947 *Ann. Phys.* **1** 333

[2] Goos F and Hänchen H 1949 *Ann. Phys.* **2** 87

[3] Schreier F, Schmitz M and Bryngdahl O 1998 *Opt. Lett.* **23** 576

[4] Shadrivov I V, Zharov A A and Kivshar Y S 2003 *Appl. Phys. Lett.* **83** 2713

[5] Li C F and Wang Q 2004 *Phys. Rev.* E **69** 055601

[6] Liu B Y and Li C F 2008 *Chin. Phys.* B **17** 3720

[7] Li C F, Zhang Y, Chen X and Zhu Q B 2008 *Chin. Phys.* B **17** 1758

[8] Liu X B, Cao Z Q, Zhu P F, Shen Q S and Liu X M 2006 *Chin. Phys. Lett.* **23** 2077

[9] Gilles H, Girard S and Hamel J 2002 *Opt. Lett.* **27** 1421

[10] Yin X, Hesselink L and Liu Z 2004 *Appl. Phys. Lett.* **85** 372

[11] Wang Y, Cao Z Q, Yu T Y, Li H G and Shen Q S 2008 *Opt. Lett.* **33** 1276

[12] Wang Y, Cao Z Q, Li H G, Jun H, Yu T Y and Shen Q S 2008 *Appl. Phys. Lett.* **93** 091103

[13] Yu T Y, Li H G, Cao Z Q, Wang Y, Shen Q S and He Y 2008 *Opt. Lett.* **33** 1001

[14] Wang Y, Li H G, Cao Z Q, Yu T Y, Shen Q S and He Y 2008 *Appl. Phys. Lett.* **92** 061117

[15] Feng Y J, Cao Z Q, Chen L and Shen Q S 2006 *Acta Phys. Sin.* **55** 4709 (in Chinese)

[16] Chen L, Cao Z Q, Shen Q S, Deng X X, Ou F and Feng Y J 2007 *J. Lightw. Technol.* **25** 539

[17] Cao Z Q, Qiu L L, Shen Q S, Dou X M and Chen Y L 1999 *Chin. Phys. Lett.* **16** 413